Hindawi
Advances in Materials Science and Engineering
Volume 2022, Article ID 3715840, 10 pages
https://doi.org/10.1155/2022/3715840

Research Article

Experimental Verification and Estimation of Fatigue Crack Growth Delay due to Single Overload

Hao Wu [1] **and Jun Zhu** [2]

[1]*School of Aerospace Engineering and Applied Mechanics, Tongji University, Shanghai 200092, China*
[2]*Nantong Taisheng Blue Island Offshore Co Ltd, Nantong 226259, China*

Correspondence should be addressed to Hao Wu; 11047@tongji.edu.cn

Received 16 June 2022; Revised 29 July 2022; Accepted 2 November 2022; Published 22 November 2022

Academic Editor: Abílio De Jesus

A novel crack driving force parameter based on the plastic zone size for overload/constant amplitude loading is proposed to estimate the fatigue crack growth (FCG) and the beneficial fatigue life due to overload. By considering the stress distribution in the plastic zone, the effective stress intensity factor (SIF) integrated from equivalent residual stress is presented. It is illustrated that the FCG rate decreases rapidly after overload and then gradually returns to the baseline FCG rate. Besides, the overload ratio R_{pic} has a significant influence on the affected length a_d and the beneficial fatigue life N_d.

1. Introduction

The fatigue life prediction is required in such applications as aerospace, automobiles, and pressure vessel industries for damage-tolerant design. As a common consequence of fatigue loading, fatigue cracks can be generated in the geometrical stress concentration areas of structures. When an overload is applied to a crack subjected to constant amplitude loading, the FCG rate could be significantly delayed, largely improving the fatigue life. Numerous works have been devoted to the study of crack propagation behavior under variable amplitude loading [1–5]. However, the estimation of the FCG rate is not a trivial issue in fatigue crack life prediction, even though overloads are well known to retard crack growth. Indeed, there is no widely accepted method, which can model all influential parameters correctly.

Generally, the fatigue life can be divided into three stages: (1) the crack nucleation, (2) the crack growth, and (3) the rupture of structure. Paris' model is one of the most frequently employed methods to predict the macro FCG rate. This empirical model postulates that the FCG rate, da/dN, is dominated by the SIF range $\Delta K = K_{max} - K_{min}$, which depends on the loads and crack length. However, this model is limited by its initial hypothesis. In recent years, it is recognized that the Paris formula based on linear elastic fracture mechanics (LEFM) cannot exactly describe the overload delay effect, where crack fatigue propagation behavior is related to the plastic zone size in front of the crack tip [6–8].

Based on the experimental results, it shows that the FCG rate is not proportional to the range of the applied stress intensity factor ΔK but rather to the effective stress intensity factor ΔK_{eff}. Indeed, only a portion of the fatigue loading cycle is effective for crack propagation, and the crack may remain closed for the other part due to elastic constraints acting on the plastically stretched material in the crack wake, according to Elber [9]. The crack closure is caused by plasticity, oxidation, roughness of the crack faces, or a phase transformation induced by mechanical loading. The plasticity-induced closure, which is particularly sensitive to loading history effects, derives from two different sources: the first is the plastic wake created by the plastic zone along the crack path, and the second is the occurrence of residual compressive stresses in front of the crack. In reality, these effects are not independent, leading to the same delay phenomenon. Therefore, the relationship between the FCG rate and the plastic stress distribution in front of the crack tip

is extremely significant for exploring crack propagation mechanisms and improving the accuracy of fatigue life prediction. In this procedure, the plasticity affected region, i.e., the monotonous plastic zone, is the origin of residual compressive stresses in front of the crack tip, which makes the subsequent cycles less effective. When the crack grows, the residual stresses are then exerted on the crack face and increase its opening level.

To reflect delay effects due to overload, Willenborg et al. [10] proposed a delay coefficient C_p associated with the plastic zone size in front of the crack tip to predict the FCG after overload. Based on the model, Bacila et al. modified the FCG model [11] using a piecewise linear function to fit the growth rate curve. Moreover, the delay effect on FCG has also been confirmed through EBSD, FIB–DIC, and FEM methods by Salvati et al. [12]. However, these empirical models need additional parameters fitted through experimental data. In addition, Wu and Carlsson [13] used a weighted residual stress intensity factor (RSIF) to quantify the crack closure effect due to the residual stress, as described in (5). And several analytical solutions for standard specimens are provided in [14–16].

In the past decades, considerable attention has been paid to the plastic zone in front of the crack tip because of its close correlation with the delay of FCG after overloading [17]. Dai et al. proposed a method that defines a plasticity-corrected SIF as a new mechanical driving force for predicting the FCG rate [18].

Fatigue crack delay caused by overload is a general phenomenon found in most engineering applications. Even though the traditional rainflow counting techniques are widely used for variable amplitude loading events, it is impossible to decide a priori, which points should be considered load reversions, decreasing the crack life prediction accuracy. Accordingly, many crack delay models are proposed based on different mechanisms. In this field, the crack closure theory has drawn many attentions, which purports that a crack will not propagate unless the crack driving force is over a specific point. However, the closure effect is still highly controversial since this effect cannot explain many of its peculiarities, such as high loading ratio conditions or high-strength steels [19–23]. Besides, many phenomenological delay models have also been proposed based on the following main hypotheses: (1) the crack length affected by overload is estimated by the plastic zone sizes, which are influenced by loading conditions; (2) the crack length corresponding to the value of the FCG rate is relative to the plastic zone size. These empirical models confirm that the plastic zone plays an important role in the quantification of the variation of the FCG rate due to overload. However, the stress distribution in the plastic zone is rarely considered in classical models. Moreover, most of the models contain complex fitting parameters, e.g., the severity coefficient in Bacila's model, both increasing the possible accumulative errors.

In this paper, with the introduction of equivalent residual stress $\overline{\sigma_{res}}$ and equivalent RSIF ΔK_{pl}, a novel crack driving force model without fitting parameters with clear physical meaning is proposed, by considering the material's hardening effect in the plastic zone near the crack tip. This model can be further incorporated with the rainflow algorithm to estimate the FCG rate under variable amplitude loading, without losing prediction accuracy. Moreover, the detailed experimental data of steels 1045 and 1080 have also been presented. A brief description of residual stress distribution ahead of the crack tip under cyclic loading is presented in Section 2. Section 3 develops a novel effective stress intensity factor, which incorporates essential delay parameters to capture the influence of a single overload. Section 4 presents the experimental setup and different applied overloads to quantify how the influential parameters affect the FCG rate and fatigue life. Proposed driving force evaluations are carried out through experimental data. Finally, conclusions are drawn in Section 5.

2. Residual Stress Distribution

LEFM presents a characteristic distribution of the tensile stress ahead of a crack tip with the following expression:

$$\sigma_y = \frac{K}{\sqrt{2\pi r}} \cos\frac{\theta}{2}\left(1 + \sin\frac{\theta}{2}\sin\frac{3\theta}{2}\right). \tag{1}$$

Generally, as shown in Figure 1, in order to meet the static equilibrium conditions, the stress reduced by the material yielding motivates the stress augmentation in the nearby elastic materials, bringing more materials to yield. Therefore, the stress distribution (dotted line) based on LEFM is transformed into the elastoplastic stress distribution (solid line). In the plane stress state, Irwin calculates the plastic zone size as follows:

$$r_p = \frac{1}{\pi}\left(\frac{K_{max}}{\sigma_0}\right)^2. \tag{2}$$

The residual stress can then be calculated through the plastic superposition method proposed by Rice. The unloading process is regarded as $\Delta\sigma = 2\sigma_0$ with a reverse plastic flow. The schematic superposed residual stress is shown in Figure 2.

Although Rice's method is widely accepted, the stress gradient in the plastic zone has not yet been considered. Actually, during cyclic loading events, the material near the crack tip plastically deforms, and the stress increases with the decrease in the distance from the crack tip. As a result, the local stress near the crack tip must be higher than the original yield stress. In other words, the neglect of material elastoplastic hardening in front of the crack tip may lead to a deviation of estimation on the fatigue crack driving force. Moreover, it can be proved that the stress near the crack tip varies from the yield stress to the strength limit according to the FEM results and physical observations [24]. Analogously, in the proposed method, the stress near the crack tip σ_1 is assumed to be equal to the average of the yield stress σ_0 and the strength limit σ_b, as follows:

$$\sigma_1 = (\sigma_0 + \sigma_b)/2. \tag{3}$$

According to equations (1)–(3), we have

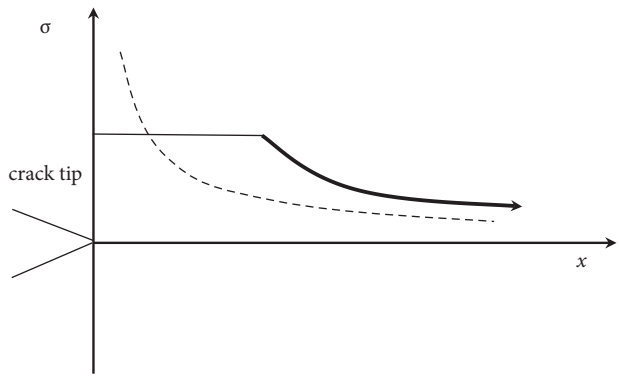

Figure 1: Stress distribution in front of the crack tip.

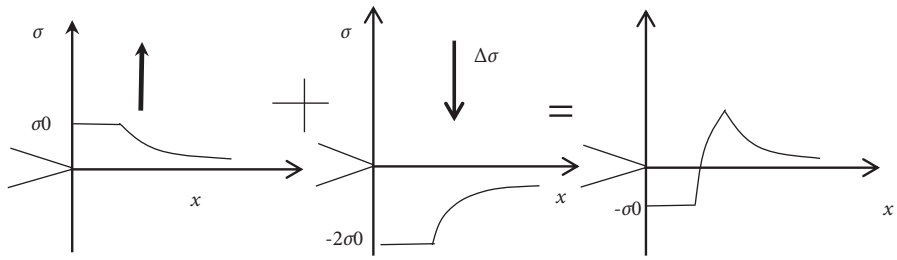

Figure 2: Schematic stress distribution by plastic stress superposition method.

$$\sigma_0(\theta = 0) = \frac{K}{\sqrt{2\pi r}}, r_p = \frac{K^2}{\pi\sigma_0^2}. \tag{4}$$

Correspondingly, due to the increased hardened stresses within the plastic zone, the yielded material causes a larger plastic zone than that estimated by Rice's method. During the unloading process, the radius of the yield plane is assumed to be fixed due to the Bauschinger effect with stress range $\Delta\sigma = 2\sigma_0$, and the plastic zone sizes can then be estimated by the following:

$$\int_0^{r_0} \sigma_y \mathrm{d}r = \frac{(\sigma_0 + \sigma_1/2 + \sigma_0)}{2} \cdot r_s = 2\sigma_0 \cdot r_t, \tag{5}$$

where the equivalent reverse radius of unloading plastic zone r_t and the equivalent radius of loading plastic zone r_s are as follows:

$$r_s = \frac{4K^2}{\pi\sigma_0(3\sigma_0 + \sigma_1)}, r_t = \frac{K^2}{2\pi\sigma_0}, \mathrm{r_{pl}} = \max(r_s, r_t). \tag{6}$$

By substituting r_t and r_s, the stress distribution in front of the crack tip after cyclic loading can then be expressed as follows:

$$\sigma = \begin{cases} \dfrac{\sigma_0 - \sigma_1}{2 \cdot r_s}\mathrm{r} + \dfrac{\sigma_0 + \sigma_1}{2}, x < r_s \\ \sigma_y(r - r_s + r_0), x \geq r_s \end{cases}, \sigma' = \begin{cases} -2\sigma_0, x < r_t \\ -\sigma_y(r - r_t + r_0), x \geq r_t. \end{cases} \tag{7}$$

where σ is the stress distribution of loading and σ' is the stress distribution of unloading.

The residual stress can then be superposed by equation (8), and the results are shown in Figure 3.

$$\sigma_{\mathrm{res}} = \sigma + \sigma'. \tag{8}$$

3. Proposed Effective SIF

Based on [13], the expression of equivalent residual stress $\overline{\sigma_{\mathrm{res}}}$ considering elastoplastic hardening in the plastic zone is correspondingly presented in (9).

$$\overline{\sigma_{\mathrm{res}}} = \int_0^{r_{\mathrm{pl}}/W} \Delta\sigma_{\mathrm{res}}\left(\frac{x}{W}\right) \cdot F(a, W) \cdot \phi\left(\frac{x}{W}\right) \mathrm{d}\frac{x}{W}. \tag{9}$$

where $\phi(x/\mathrm{W})$ is a weight function.

According to Qylafku's results [25], the weight function $\phi(x/W)$ is a monotonically decreasing function and relates to the geometry of specimens, having the following characteristics:

$$\begin{cases} 0 \leq \phi\left(\dfrac{x}{W}\right) \leq 1 \\ \phi\left(\dfrac{x}{W}\right) = 1 \end{cases}. \tag{10}$$

A power exponential function is proposed as follows:

$$\phi\left(\frac{x}{W}\right) = e^{-D \cdot \frac{x}{W}}, F(a, W) = \frac{4\pi D}{f(a/W) \cdot \sqrt{\pi a/W_0}}, \tag{11}$$

where D has the expression

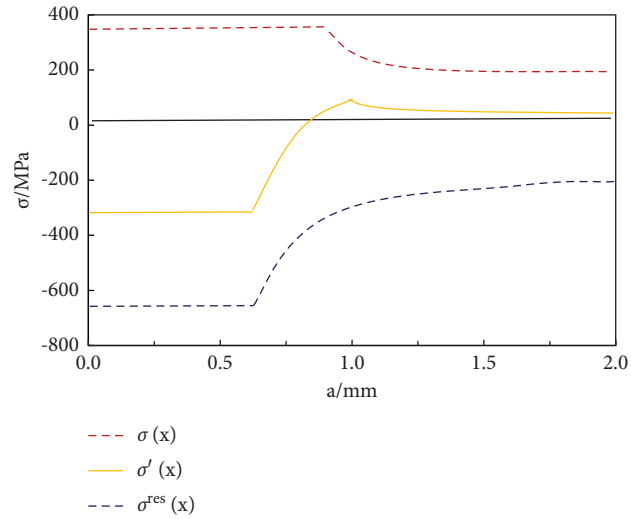

Figure 3: Superposed residual stress distribution considering elastoplastic hardening in plastic zone.

$$D = \frac{W}{W_0}, \tag{12}$$

with $W_0 = 2.5$ mm, which is the baseline width of the specimen. In addition, f is a dimensionless function with the following equation for CT specimens [26]:

$$f(\alpha) = \frac{(2+\alpha)\left(0.886 + 4.64\alpha - 13.33\alpha^2 + 14.72\alpha^3 - 5.6\alpha^4\right)}{\left(1-\alpha^{3/2}\right)}, \alpha = \frac{a}{W} \tag{13}$$

Therefore, equivalent RSIF ΔK_{res} based on $\Delta\overline{\sigma_{\text{res}}}$ is given by the following:

$$\Delta K_{res} = \sqrt{\pi a} \cdot \Delta\overline{\sigma_{res}} \cdot f\left(\frac{a}{W}\right) = 4\pi \frac{W}{\sqrt{W_0}} \cdot \int_0^{r_{pl}/W} \Delta\sigma_{res}\left(\frac{x}{W}\right) \cdot e^{-\frac{W}{W_0}\cdot\frac{x}{W}} d\frac{x}{W}. \tag{14}$$

Obviously, ΔK_{pl} is mainly dependent on load amplitude, which can reflect the difference between constant and overloaded loading events. ΔK_{eff} is derived from ΔK_{res}, as described in equations (15) and (16). Note that $\Delta K_{\text{res}}^{\text{const}}$ and $\Delta K_{\text{res}}^{\text{overload}}$ are RSIF under constant and overloaded loading, respectively. And $\Delta K_{\text{res}}^{\text{overlapping}}$ is the overlapping part of $\Delta K_{\text{res}}^{\text{const}}$ and $\Delta K_{\text{res}}^{\text{overload}}$.

$$\Delta K_{\text{pl}} = \Delta K_{\text{res}}^{\text{const}} + \Delta K_{\text{res}}^{\text{overload}} - \Delta K_{\text{res}}^{\text{overlapping}}. \tag{15}$$

Finally, ΔK_{eff} can be obtained by substituting Eq. (7), (8), and (14) into (15), given by the following:

$$\Delta K_{\text{eff}} = \Delta K - \Delta K_{\text{pl}}. \tag{16}$$

Moreover, the crack length affected by delay a_d can be calculated by (17).

$$a_d = r_{\text{pl}}^{\text{overload}} - r_{\text{pl}}^{\text{const}}. \tag{17}$$

One advantage of this method is that it can reach rather quickly the calculation of the affected delay cycle number N_d. Indeed, it is very simple to get the characteristic and essential delay parameters by the integral method. In summary, to quantify the influence of the plastic zone on FCG life after a single overloading, the proposed effective SIF can be used in the prediction of FCG rate based on the traditional form of the Paris formula, as described in (18).

$$\frac{\mathrm{d}a}{\mathrm{d}N} = C\left(\Delta K - \Delta K_{\text{pl}}\right)^m. \tag{18}$$

The delay cycles number N_d is given by the following expression:

$$N_d = \int_{a_0}^{a_d} \frac{1}{(\mathrm{d}a/\mathrm{d}N)}\,\mathrm{d}a. \tag{19}$$

The integration starts at the position a_0 where the overload occurs.

4. Experimental Investigation and Discussions

To verify the prediction capabilities of the presented estimated framework, compact tension (CT) specimens made of 1045 and 1080 steel are employed for the fatigue crack propagation study, see Figure 4. The recommendation for the dimensions of specimens in the ASTM standard [22] is adopted with a thickness $B = 15$ mm and a width $W = 80$ mm. In order to characterize the mechanical properties, tensile tests are performed on cylindrical specimens (diameter $d = 11$ mm). The results illustrated in Table 1 reveal two yield stress families: low (1045) and high (1080). The

Figure 4: CT specimen mounted in a fatigue machine.

Table 1: Mechanical properties of tested steels.

Material	σ_0 0.2% (MPa)	σ_b (MPa)	E (GPa)	K (MPa)	n
1045	340	710	208	1117	0.25
1080	978	1249	207	729	0.15

baseline SIF range ΔK of these specimens can be calculated by equation (20) [27]:

$$\Delta K = \frac{\Delta P}{B\sqrt{W}}\left[\frac{(2+\alpha)\left(0.886 + 4.64\alpha - 13.33\alpha^2 + 14.72\alpha^3 - 5.6\alpha^4\right)}{\left(1-\alpha^{3/2}\right)}\right], \alpha = \frac{a}{W}. \tag{20}$$

Fatigue tests are performed under constant ΔK with a stress ratio of $R = 0.1$ in order to maintain the same baseline plastic zone sizes with a loading frequency of 15 Hz. During each test, a single overload cycle, as shown in Figure 5 is applied with a loading frequency of 0.1 Hz. Table 2 specifies the parameters for two materials with five different overload ratios R_{pic}.

The curve of ΔK_{eff} versus crack length under the overload ratio $R_{pic} = 1.5$, 2, and 2.5 is presented in Figure 6. It can be found that after overloading, ΔK_{eff} is reduced to a minimum value and gradually recovers to the baseline SIF value. Moreover, the minimum value of ΔK_{eff} decreases with the increase of the overload ratio R_{pic}. And the result can well interpret the delay hysteresis of the overloading, which means the FCG rate is not immediately reduced to the lowest point when the overloading occurs but gradually reduced to the lowest rate, which depends on the plastic zone size in front of the crack tip.

To validate the proposed empirical driving force parameter in fatigue crack life prediction, the estimated overloaded FCG rate is compared with the experimental data for two materials with the same overload ratio $R_{pic} = 2.5$, as shown in Figure 7. It is illustrated that this proposed method leads to an acceptable description of the two stages of the FCG rate after a single overloading because the position of the lowest point, the affected delay length, and the curve tendency are all within a reasonable error range with respect to the experimental results.

Moreover, for the material with low yield strengths such as 1045, the a_d is relatively longer and the recovery rate is much higher than that of materials with high yield strength such as 1080. Similar phenomena are also found in Louah's results [23], which can prove that the crack closure effect is weakly influenced by the overloaded cycle in the case of high-strength steels.

The estimated FCG rates with different overload ratios R_{pic} for two materials are presented in Figure 8. According to the tendency of the curves, it can be concluded that the delay effect of the FCG rate is mainly dominated by R_{pic}, which manifests in the form of a convex function. It means that the curves drop rapidly to the lowest point immediately after overloading and are followed by gradual returns to the

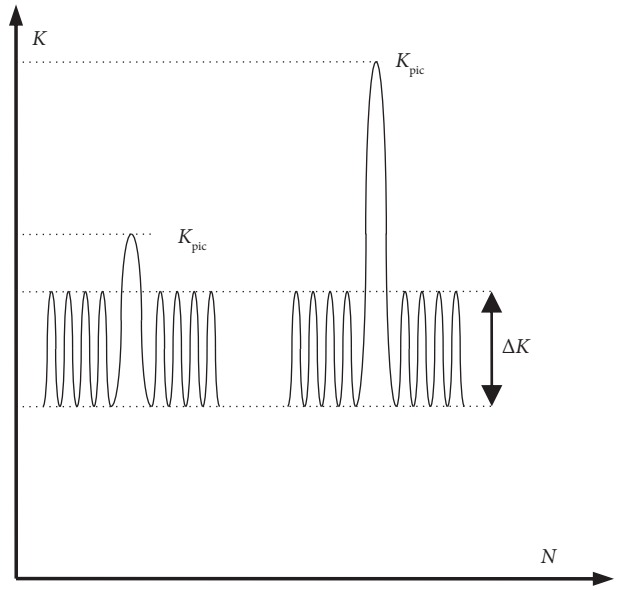

Figure 5: Schematic illustration of applied loading.

Table 2: Loading parameters.

Steel 1045				Steel 1080			
R_{pic}	K_{pic}	ΔK	R	R_{pic}	K_{pic}	ΔK	R
1.5	39	23.4	0.1	1.5	42.7	25.6	0.1
1.8	46.8	23.4	0.1	1.8	51.3	25.6	0.1
2	52	23.4	0.1	2	57	25.6	0.1
2.2	57.2	23.4	0.1	2.2	62.7	25.6	0.1
2.5	65	23.4	0.1	2.5	71.2	25.6	0.1

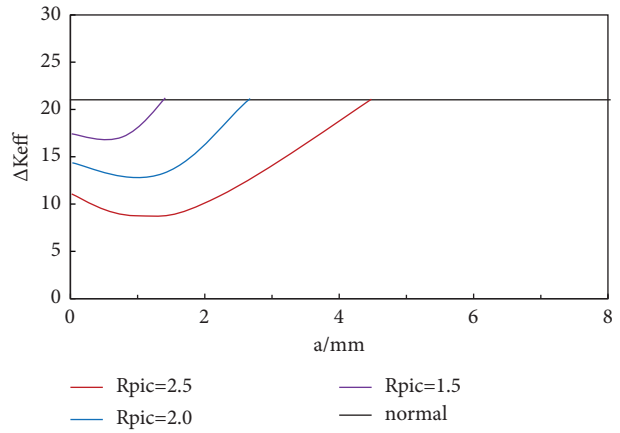

Figure 6: Variation of ΔK_{eff} with crack growth.

baseline rate, which is influenced by the stress distribution in the plastic zone.

The estimated and observed fatigue lives for materials 1045 and 1080 are listed in Table 3. Moreover, the comparison of the estimated and experimental results is plotted in Figure 9. It can be found that the prediction results correlated well with the experimental data, as all points fall within a factor of 2 time scatter band. Compared to the traditional empirical models, the stress hardening in front of the crack tip is considered in the proposed method, which can more reasonably quantify the overload delay effect. It is necessary to point out that for the proposed method, which has no fitting parameter in the calculation, the agreement of the predictions at diverse levels of the FCG rate, overload level, affected length, and fatigue life is remarkable.

Besides, two empirical FCG delay models are also used to compare the fatigue life prediction capability of the proposed

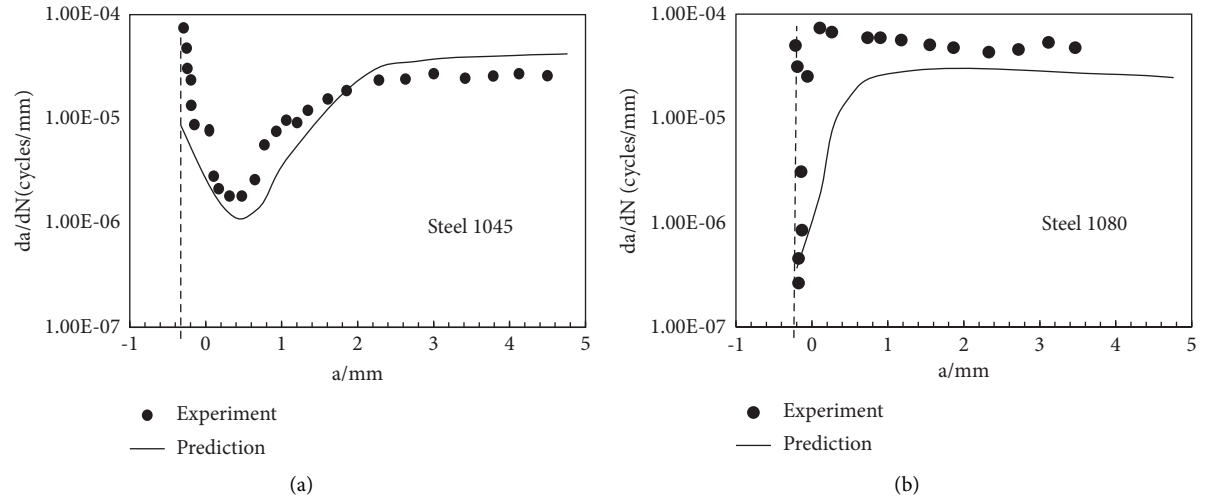

Figure 7: Comparison between the experimental data and estimated results for FCG rate of 1045 (a) and 1080 (b).

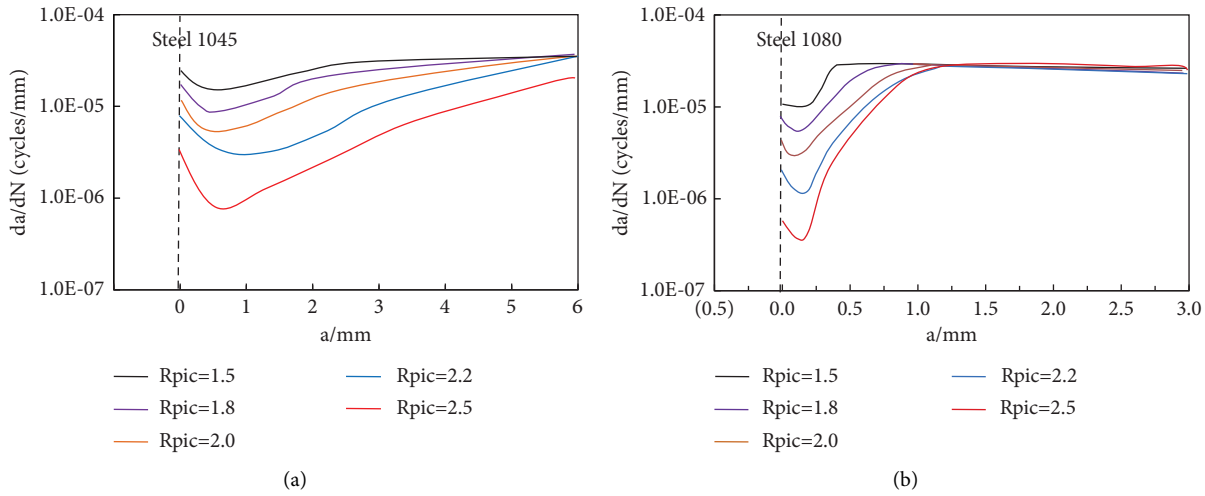

Figure 8: Estimated FCG rate curve with different R_{pic} for steel 1045 (a) and 1080 (b).

Table 3: Predicted and experimental fatigue life for steel 1045 and 1080.

R_{pic}	Steel 1045		Steel 1080	
	Predicted life (1000 cycles)	Experiment life (1000 cycles)	Predicted life (1000 cycles)	Experiment life (1000 cycles)
1.5	75.2	51.6	6.16	9.4
1.8	159.9	150.3	11.0	19.6
2	242.3	206.1	13.9	24.7
2.2	382.1	398.6	25.3	41.1
2.5	630.1	765.6	83.8	133.5

method under the same conditions. The first one is based on the weight function solutions proposed by Wu [13], and the second one is based on the modified equivalent inclusion theory proposed by Li [17, 28].

The life prediction results of these two methods are given in Table 4.

Figures 10 and 11 illustrate a comparison of fatigue life predictions with the experimental results based on Wu's and Li's methods. The correlation coefficient R_c and mean square error (MSE) defined by Mohanty [29] as shown in (21) are adopted to describe the deviation between the predicted and experimental results, detailed in Table 5. It can be found that, for overload events, these three methods have strong applicability in fatigue life prediction. However, according to R_c and MSE, the proposed method in this paper has much higher accuracy and better stability.

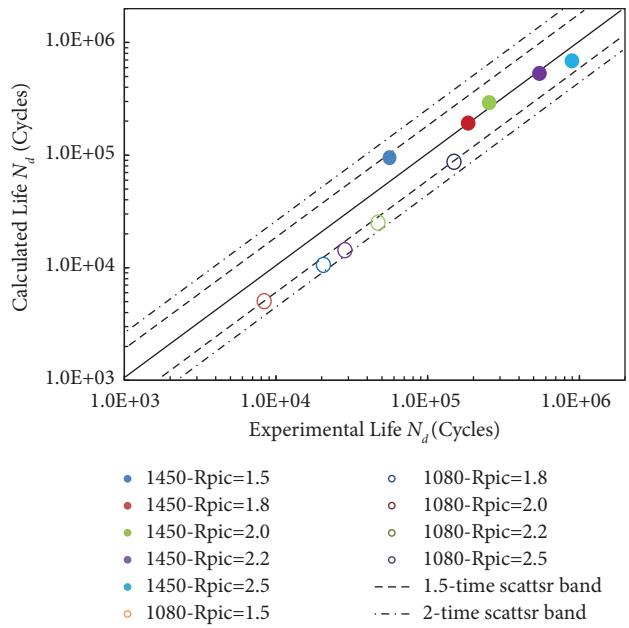

Figure 9: Comparison between experimental data and fatigue life estimated by the proposed method.

Table 4: Fatigue life prediction by Wu's and Li's methods.

Rpic	Steel 1045		Steel 1080	
	Wu's methods (1000 cycles)	Li's methods (1000 cycles)	Wu's methods (1000 cycles)	Li's methods (1000 cycles)
1.5	51.3	23	14	4.8
1.8	105.6	89	31.232	20
2	145.5	128	50.162	52
2.2	197.3	335	84.406	112
2.5	283.2	1083	119.65	2518

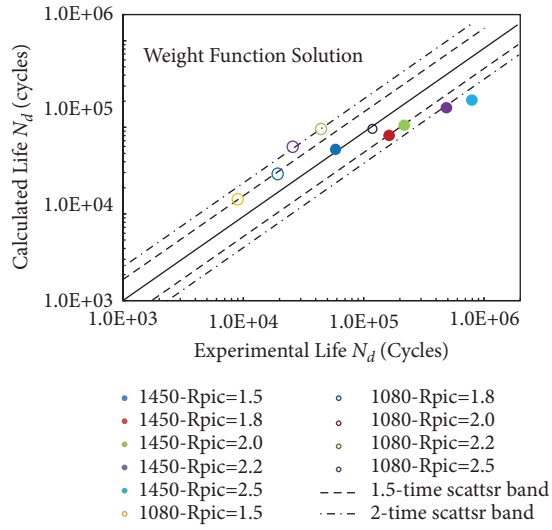

Figure 10: Comparison between experimental data and fatigue life estimated by Wu's method.

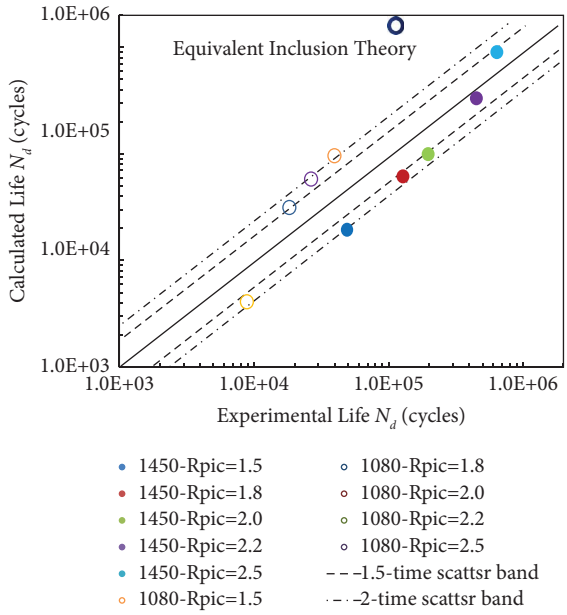

Figure 11: Comparison between experimental data and fatigue life estimated by Li's method.

Table 5: R_c and MSE.

Methods	Steel 1045		Steel 1080	
	R_c	MSE/1k	R_c	MSE/1k
Proposed method	0.9949	4.118	0.9997	0.6
Wu's method	0.9765	55.775	0.9063	0.574
Li's method	0.9803	23.09	0.9814	1138

$$\begin{cases} R_c = \dfrac{\sum_{i=1}^{n}\left(\left(N_{ex}-N'_{ex}\right)\left(N_{pr}-N'_{pr}\right)\right)}{\sqrt{\sum\left(N_{ex}-N'_{ex}\right)^2\left(N_{pr}-N'_{pr}\right)^2}} \\ \text{MSE} = \dfrac{\sum_{i=1}^{n}\left(N_{ex}-N_{pr}\right)^2}{n} \end{cases}. \quad (21)$$

5. Conclusions

The delay effect of overloading on the FCG rate for different materials has been studied in the paper. By taking into account of the residual stress in the plastic zone in front of the crack tip, a novel empirical crack driving force parameter with no need for fitting parameters is presented, and the influenced FCG rate is used to estimate the beneficial fatigue life. A series of fatigue experiments with five overload ratios R_{pic} for two materials are performed. The conclusions below can be drawn:

(1) The residual compressive stress in the plastic zone in front of the crack tip due to overloading is the main reason for FCG delay;

(2) After a single overloading, the FCG rate curve will gradually decrease to the lowest point, and then slowly return to the baseline rate in the form of a convex function;

(3) The higher the overload ratio R_{pic} value is, the less is the minimum FCG rate after overloading;

(4) The proposed crack driving force parameter, taking into account of the elastoplastic hardening in the plastic zone, can be used to effectively predict the beneficial fatigue life due to overloading, which is validated by comparing the predicted and experimental results.

Abbreviations

σ_0: Yield strength
σ_0: Stress close to crack tip
σ_{res}: Equivalent residual stress
σ_{res}: Residual stress distribution in front of the crack tip
a_0: Crack length where overload occurs
a: Crack length
a_d: Crack length affected by delay
K_c: Fracture toughness
ΔK_{eff}: Effective stress intensity factor
K_{res}: Equivalent residual stress intensity factor
N_d: Crack initiation life
R_{pic}: Overload ratio
r_s: Equivalent radius of loading plastic zone
r_t: Equivalent reverse radius of unloading plastic zone
r_p: Irwin radius of plastic zone
r_{pl}: Radius of the plastic zone in front of the crack tip
RSIF: Residual stress intensity factor
SIF: Stress intensity factor
W: Specimen width.

Data Availability

The data that support the findings of this study are available from the corresponding author, Hao Wu, upon reasonable request.

Conflicts of Interest

The authors declare that they have no conflicts of interest.

Acknowledgments

This work was supported by the National Natural Science Foundation of China (No. 11972255) and the Shanghai Natural Science Foundation (No. 19ZR1459000).

References

[1] X. P. Huang, M. Torgeir, and W. C. Cui, "An engineering model of fatigue crack growth under variable amplitude loading," *International Journal of Fatigue*, vol. 30, no. 1, pp. 2–10, 2008.

[2] P. C. Paris and F. A. Erdogan, "A critical analysis of crack propagation laws," *Journal of Basic Engineering*, vol. 85, no. 4, pp. 528–533, 1963.

[3] A. El Malki Alaoui, D. Thevenet, and A. Zeghloul, "Short surface fatigue cracks growth under constant and variable

amplitude loading," *Engineering Fracture Mechanics*, vol. 76, no. 15, pp. 2359–2370, 2009.

[4] S. B. Singh and R. Kumar, "A study of fatigue crack growth is1020 steel under constant-amplitude loading," *International Journal of Pressure Vessels and Piping*, vol. 52, no. 2, pp. 177–188, 1992.

[5] R. G. Forman, V. E. Kearney, and R. M. Engle, "Numerical analysis of crack propagation in cyclic-loaded structures," *Journal of Basic Engineering*, vol. 89, no. 3, pp. 459–463, 1967.

[6] S. Dinda and D. Kujawski, "Correlation and prediction of fatigue crack growth for different R-ratios using Kmax and ΔK+ parameters," *Engineering Fracture Mechanics*, vol. 71, no. 12, pp. 1779–1790, 2004.

[7] J. P. Belnoue, T. S. Jun, F. Hofmann, B. Abbey, and A. M. Korsunsky, "Evaluation of the overload effect on fatigue crack growth with the help of synchrotron XRD strain mapping," *Engineering Fracture Mechanics*, vol. 77, no. 16, pp. 3216–3226, 2010.

[8] R. C. Mcclung and H. Sehitoglu, "On the finite element analysis of fatigue crack closure-1. Basic modeling issues," *Engineering Fracture Mechanics*, vol. 33, no. 2, pp. 237–252, 1989.

[9] W. Elber, "Fatigue crack closure under cyclic tension," *Engineering Fracture Mechanics*, vol. 2, no. 1, pp. 37–45, 1970.

[10] J. Willenborg, R. M. Engle, and H. A. Wood, *A Crack Growth Retardation Model Using an Effective Stress Concept*, Defense Technical Information Center, 1971.

[11] A. Bacila, X. Decoopman, G. Mesmacque, M. Voda, and V. Serban, "Study of underload effects on the delay induced by an overload in fatigue crack propagation," *International Journal of Fatigue*, vol. 29, no. 9-11, pp. 1781–1787, 2007.

[12] E. Salvati, S. O'Connor, T. Sui, D. Nowell, and A. Korsunsky, "A study of overload effect on fatigue crack propagation using EBSD, FIB-dic and FEM methods," *Engineering Fracture Mechanics*, vol. 167, pp. 210–223, 2016.

[13] X. R. Wu and A. J. Carlsson, *Weight Functions and Stress Intensity Factor Solutions*, oxford, 1991.

[14] W. Xu, X. R. Wu, and Y. Yu, "Weight function, stress intensity factor and crack opening displacement solutions to periodic collinear edge hole cracks: periodic collinear edge hole cracks," *Fatigue and Fracture of Engineering Materials and Structures*, vol. 40, no. 12, pp. 2068–2079, 2017.

[15] W. Xu, X. R. Wu, Y. Yu, and Z. H. Li, "A weight function method for mixed modes hole-edge cracks," *Fatigue and Fracture of Engineering Materials and Structures*, vol. 41, pp. 223–234, 2018.

[16] X. R. Wu, X. C. Zhao, W. Xu, and D. H. Tong, "Discussions on weight functions and stress intensity factors for radial crack(s) emanating from a circular hole in an infinite plate," *Engineering Fracture Mechanics*, vol. 192, pp. 192–204, 2018.

[17] P. Zhu, L. Yang, Z. Li, and J. Sun, "The shielding effects of the crack-tip plastic zone," *International Journal of Fracture*, vol. 161, no. 2, pp. 131–139, 2010.

[18] P. Dai, S. Li, and Z. Li, "The effects of overload on the fatigue crack growth in ductile materials predicted by plasticity-corrected stress intensity factor," *Engineering Fracture Mechanics*, vol. 111, pp. 26–37, 2013.

[19] J. T. P. Castro, M. A. Meggiolaro, and J. A. O. González, "Can ΔKeff be assumed as the driving force for fatigue crack growth?" *Frattura Ed Integrità Strutturale*, vol. 9, pp. 97–104, 2015.

[20] A. Vasudeven, K. Sadananda, and N. Louat, "A review of crack closure, fatigue crack threshold and related phenomena," *Materials Science and Engineering A*, vol. 188, no. 1-2, pp. 1–22, 1994.

[21] S. E. Ferreira, J. T. P. d. Castro, M. A. Meggiolaro, and A. C. d. Oliveira Miranda, "Crack closure effects on fatigue damage ahead of crack tips," *International Journal of Fatigue*, vol. 125, pp. 187–198, 2019.

[22] S. C. Forth, M. A. James, W. M. Johnston, and J. C. Newman, "Anomolous fatigue crack growth phenomena in high-strength steel," *Crack growth threshold testing*, 2013.

[23] M. Louah, *I+II Mixed Mode Fatigue Crack of Brazilian Disc, Thesis in French*, University of Technology of Compiegne, 1980.

[24] J. C. Newman, "A crack-closure model for predicting fatigue crack growth under aircraft spectrum loading," in *Methods and Models for Predicting Fatigue Crack Growth under Random Loading*, J. Chang and C. Hudson, Eds., pp. 53–84, Hampton, VA, United States, 1981.

[25] G. Qylafku, Z. Azari, and N. Kadi, "Application of a new model proposal for fatigue life prediction on notches and key-seats," *International Journal of Fatigue*, vol. 21, no. 8, pp. 753–760, 1999.

[26] *Standard Test Method for Plane-Strain Fracture Toughness of Metallic Materials*, ASTM E399, 1983.

[27] *Standard Test Method for Measurement of Fatigue Crack Growth Rates*, ASTM E 647, 1988.

[28] Z. H. Li and J. Y. Duan, "The effect of a plastically deformed zone near crack tip on the stress intensity factors," *International Journal of Fracture*, vol. 117, no. 4, pp. 29–34, 2002.

[29] J. R. Mohanty, T. K. Mahanta, A. Mohanty, and D. Thatoi, "Prediction of constant amplitude fatigue crack growth life of 2024 t3 al alloy with r-ratio effect by GP," *Applied Soft Computing*, vol. 26, pp. 428–434, 2015.